

Nonlinear dielectric response in glass formers: Restoring forces and avoided spin-glass criticalityEric Bertin¹ and François Ladieu²¹*Univ. Grenoble Alpes, CNRS, LIPhy, 38000 Grenoble, France*²*SPEC, CEA, CNRS, Université Paris-Saclay, CEA Saclay, Bat 772, 91191 Gif-sur-Yvette Cedex, France*

(Received 7 December 2023; revised 4 April 2024; accepted 4 June 2024; published 28 June 2024)

Experimental measurements of nonlinear dielectric response in glass formers like supercooled glycerol or propylene carbonate have been interpreted as providing evidence for a growing thermodynamic length scale when lowering temperature. A heuristic picture based on coherently flipping “superdipoles” with disordered internal structure has been argued to capture the essence of the experimentally reported behavior, pointing to the key role of effectively disordered interactions in structural glasses. We test these ideas by devising an explicit one-dimensional model of interacting spins incorporating both the spin-glass spirit of the superdipole argument and the necessary long-time decorrelation of structural disorder, encoded here in a slow dynamics of the coupling constants. The frequency-dependent third-order response of the model qualitatively reproduces the typical humped shape reported in experiments. The temperature dependence of the maximum value is also qualitatively reproduced. In contrast, the humped shape of the third-order response is not reproduced by a simple kinetically constrained spin model with noninteracting spins. To rationalize these results, we propose a two-length-scale scenario by distinguishing between the characteristic length of dynamical heterogeneities and a rigidity length that accounts for the local tendency of spins to flip coherently as a block, in the presence of interactions. We show that both length scales are identical in the kinetically constrained spin model, while they have significantly different dynamics in the model of interacting spins.

DOI: [10.1103/PhysRevE.109.064156](https://doi.org/10.1103/PhysRevE.109.064156)**I. INTRODUCTION**

Understanding the origin of the very fast increase of the relaxation time τ_α of molecular glass formers over a moderate temperature range remains a challenging task for condensed matter physics [1,2]. As a consequence the glass transition temperature T_g is merely defined by $\tau_\alpha(T_g) = 100\text{s}$. Experimentally, the glass transition has been studied by a vast range of techniques [3], ranging from nuclear magnetic resonance [4] to dielectric spectroscopy [5], neutron diffraction [6,7], optical techniques [8–11], and even atomic force microscopy [12]. As each technique specifically probes some degrees of freedom, comparing the experimental results is of great interest; see, e.g., [13]. This comparison reveals that all of them are well coupled, apart from one exception which is physically understood [13,14]. Indeed, upon cooling, they exhibit a similar characteristic timescale, called the α relaxation time, which governs, e.g., both dielectric spectra—probing rotation of molecules—and viscosity behavior—probing the mechanical response of molecules. Furthermore, it has been gradually established [1,2] that, in supercooled liquids, relaxation happens through groups of molecules whose dynamics is correlated: at a given instant, some of these groups are much faster than others, hence their name “dynamical heterogeneities” (DH). Yet, despite the impressive number of experimental studies characterizing the glass transition, the origin of this extremely fast viscous slow down and of DH’s remains debated [1,2], and opposite theories—either *static* or *dynamic*—claim to account for the phenomenology of glass formers.

According to static theories [15,16] formation of glasses is primarily driven by the emergence of growing static

correlations, capturing the idea of “amorphous order,” namely, nonperiodic molecular configurations with low free energy. In this view, the material gradually solidifies as these low-energy local molecular packings become harder to relax or to perturb when temperature decreases. In dynamic theories instead [17,18], structural information plays little role, and emphasis is placed on the existence of local mobile defects that can relax the entire configuration. This view is captured by simple kinetically constrained models (KCMs) [19], where the rarefaction of diffusive localized defects at low temperature is introduced as a minimal ingredient. In this approach, DHs emerge because a single defect has to relax many molecules as it moves, thus building spatial correlations between relaxation events.

Given the ability of KCMs to account for the main observed dynamical features of real glass formers [20], do we really *need* the complex notion of amorphous ordering, which is imported from the field of spin glasses in high dimensions, to get a realistic theory of the molecular glass transition [21]? Despite the considerable number of numerical works highlighting the presence of amorphous ordering in *model* glass formers (see, e.g., [22,23]), the question remains vividly debated, as shown by recent works [24] and [25] whose titles express opposed views on this central question. This controversy comes from the fact that we do not have a single experimental observable whose behavior is unanimously ascribed to the growth of amorphous order upon cooling. Nearly two decades ago, it was argued [26] that, on general grounds, the jump of the specific heat around T_g was not consistent with KCM models; but this was contested, a few months later, by elaborating a refined KCM [27] showing a behavior

reasonably consistent with experiments. This paper is devoted to another observable, namely, the nonlinear dielectric susceptibility, which, in the last decade, has been argued to provide evidence for amorphous ordering, as we now explain.

Experimental measurements of nonlinear dielectric response in glass formers like supercooled glycerol or propylene carbonate have been consistently reported by several groups since 2010 [28–32]. The experimental behavior was found consistent with a theoretical prediction [33,34] inspired by the amorphous ordering occurring in spin glasses, and adapted to the realm of molecular glass formers (where the configurational entropy is nonzero). Because in spin glasses, the presence of amorphous order is evidenced by the divergence of the nonlinear (magnetic) susceptibility at the critical temperature T_{SG} , the idea guiding the prediction of Refs. [33,34] was to use the nonlinear (dielectric) susceptibility as a probe of amorphous order in molecular liquids.

The main experimental outcomes were twofold: first, it was found that nonlinear responses of third order, χ_3 [28–31], and of fifth order, χ_5 [35], have a characteristic humped shape when plotted as a function of frequency, and, second, that their maximum value *grows when temperature is lowered*, or pressure increased [31]. Because this anomalous increase upon cooling is reminiscent of the spin-glass behavior, it was interpreted as a measure of a dynamical length scale ℓ_{NonLin} directly revealing the growth of amorphous order in the glass former upon cooling. This interpretation was reinforced by showing that one accounts for the dramatic increase of relaxation time provided the free energy barrier grows typically as a power law of ℓ_{NonLin} [28–31]. From these measurements, a heuristic picture inspired by spin-glass physics has emerged [36,37], namely, the idea that global relaxation results from the coherent relaxation of “rigid superdipoles” having a size approximately equal to ℓ_{NonLin} . Quite importantly, these superdipoles have a disordered and essentially frozen internal structure in terms of the microscopic dipoles, and their relaxation as rigid blocks is key to rationalize the experimentally observed behavior of the nonlinear response as a function of frequency and temperature [32,38], including work done previously in another perspective [39–41]. This is why, it was finally argued [35,42], that such a coherent relaxation of superdipoles of increasing size (when temperature is lowered) implies that thermodynamic aspects play an important role in the relaxation of glass formers. As a consequence of this line of thought, KCMs are not expected to be sufficient to account for the nonlinear responses of supercooled liquids, despite their ability to account for DHs at zero applied field. However, no consensus has been reached yet in the glass community regarding this issue [43,44], and, furthermore, recent extensive numerical simulations of low-temperature model glass formers indicate that dynamic facilitation could still play a major role close to T_g [45,46].

This lack of consensus is partly due to the fact that nonlinear responses are notoriously difficult to evaluate, up to the point that explicit calculations are possible only in oversimplified frameworks, such as phenomenological models [36,37], or simplified models where the mechanism leading to a supercooled state plays no direct role [47–50]. Moving to the theories accounting for the glass transition in itself, whatever the viewpoint adopted about the importance of thermodynamics

aspects, the proposed theoretical reasonings mostly rely on general and plausible arguments [38,42,44] and not on fully explicit calculations. Although quite successful in terms of comparison with the experimental data [28,35,44], these general arguments leave a number of important questions open, such as: Which type of interactions between microscopic dipoles could generate an emerging phenomenology in terms of superdipoles with disordered but rigid internal structure? Can a notion of “amorphous order” be consistently characterized in an explicit model out of the superdipole picture? How can these superdipoles melt in the long-time regime to recover a trivial nonlinear response at very low frequency, and thereby reproduce the humped shape of nonlinear responses (in particular the third order one)?

In this paper we evaluate the nonlinear response in explicit model glass formers with many microscopic degrees of freedom, where glassiness emerges directly from the collective dynamics. We consider here minimal models retaining only polarization degrees of freedom, and not translational degrees of freedom. Our focus is thus specifically on the analysis of the nonlinear response to an external field coupled to the polarization degrees of freedom, and not on the mechanical properties of glass formers. For the sake of simplicity, we restrict ourselves to one-dimensional models where polarization degrees of freedom are described as Ising spins. This minimal setting is aimed to determine robust qualitative features of the nonlinear response that could be shared by more realistic glassy models. Our goal is in particular to investigate the role of a putative amorphous order in the humped shape of the nonlinear response.

More in detail, we propose two explicit one-dimensional models, which both cannot have any long-range thermodynamic order at finite temperature. Our two models differ only about the importance of interactions between effective degrees of freedom, and we compare their nonlinear responses in frequency and temperature. On one side we devise an explicit one-dimensional model of interacting spins incorporating both the spin-glass spirit of the superdipole argument, and the necessary long-time decorrelation of structural disorder, encoded here in a slow dynamics of the coupling constants between neighboring spins. We find that the frequency-dependent third-order response of the model qualitatively reproduces the typical humped shape reported in experiments, and that the static third-order response is that of noninteracting spins. The temperature dependence of the maximum value is also qualitatively reproduced. We compare step by step these results with those obtained with our second model, which is a simple kinetically constrained spin model inspired by the Fredrickson-Andersen model. We find that the cubic response of the kinetically constrained model monotonically decreases as a function of frequency. These results are rationalized through a two-length scale scenario, which distinguishes between the characteristic length of dynamical heterogeneities and a rigidity length, which monitors the effect of interactions. Our results indicate that both length scales are identical in the kinetically constrained spin model, while they have significantly different dynamics in the model of interacting spins. These results provide some quantitative evidence in favor of the important role played by the growth of amorphous order in glass formers upon cooling.

II. STOCHASTIC SPIN MODELS

A. Disordered spin model with slowly evolving couplings

1. Spin dynamics

We consider a one-dimensional spin model with N spins $S_i = \pm 1$ ($i = 1, \dots, N$), with periodic boundary conditions ($S_{N+1} \equiv S_1$). An external field $E(t)$, playing the role of the electric field in the experiment, is applied. Neighboring spins S_i and S_{i+1} on the lattice interact via a link-dependent coupling constant $J_{i,i+1}$. The time-dependent Hamiltonian of the model reads

$$H(t) = - \sum_{i=1}^N J_{i,i+1} S_i S_{i+1} - E(t) \sum_{i=1}^N S_i. \quad (1)$$

The stochastic dynamics is constrained by the detailed balance property, valid for a static field $E(t) = E_0$. More specifically, spins are assumed to obey a stochastic reversal dynamics satisfying detailed balance with respect to the equilibrium distribution associated with the Hamiltonian H (corresponding to a static field E_0), $P_{\text{eq}} \propto e^{-\beta H}$, where $\beta = 1/k_B T$ is the inverse temperature. The probability per unit time to flip a spin is chosen according to the Glauber rate

$$W(-S_i | S_i) = \frac{\nu_0}{1 + e^{\beta \Delta H_i^S}}, \quad (2)$$

where ΔH_i^S is the energy change induced by the reversal of the spin S_i , and where ν_0 is the characteristic attempt frequency of the spin dynamics. We further assume that the definition (2) of the transition rates remains valid for a time-dependent field $E(t)$, leading to time-dependent transition rates: this is well justified (see, e.g., Chap. 14 of Ref. [51]) in our case where the frequency of the field is much smaller than ν_0 .

2. Coupling dynamics

In the form (1), the Hamiltonian is very similar to that of a spin-glass model. This spin-glass-like form of the Hamiltonian is motivated by the standard heuristic argument describing a dielectric glass former as a set of superdipoles, each one being made of frozen and disordered arrangement of electric dipoles [36] (see also Sec. V A). This phenomenological argument, deeply rooted in the spin-glass physics, predicts a divergence of the nonlinear dielectric responses when a rigidity length, characterizing the size of superdipoles, increases. The argument also correctly predicts the absence of divergence for the linear dielectric response.

In spite of this qualitative success, one of the difficulties with the above heuristic argument is that it does not describe how the nonlinear dielectric response becomes small again at very low frequencies. Intuitively, this is the regime where the disorder inside the superdipoles unfreezes due to, e.g., the fact that molecules are anisotropic objects which mutual interaction depends onto their relative orientation; for example the dipole-dipole interaction changes its sign depending on the angle between two molecular dipoles. Therefore as the system relaxes, the mutual orientations of molecules changes and their interactions are modified and may even change sign. Assuming that couplings $J_{i,i+1}$ in our model play a role similar to the interactions between molecules—which is implicit in Eq. (1)—and are thus key to the glass transition, the couplings

$J_{i,i+1}$ would also be expected to change their sign in the long run. To include this effect explicitly in the model, we assume that the coupling constants $J_{i,i+1}$ are not completely frozen but have a slow dynamics, on a timescale much longer than the timescale of the spin dynamics (see also [52] for a closely related model in the context of neural networks). For simplicity, we choose bivalued coupling constants $J_{i,i+1} = \pm J_0$, and assume a stochastic reversal dynamics $J_{i,i+1} \rightarrow -J_{i,i+1}$ with a transition rate satisfying detailed balance with respect to the equilibrium distribution P_{eq} . The probability per unit time to reverse the sign of the coupling constant $J_{i,i+1}$ is assumed to be

$$W(-J_{i,i+1} | J_{i,i+1}) = \frac{\nu_1}{1 + e^{\beta \Delta H_{i,i+1}^J}}, \quad (3)$$

where $\Delta H_{i,i+1}^J$ is the energy change induced by the reversal of the coupling constant $J_{i,i+1}$, and where ν_1 is the characteristic attempt frequency of the dynamics. As we expect coupling constants to evolve on much larger timescales than the spins, we assume that $\nu_1 \ll \nu_0$, so that the coupling constants appear as essentially frozen on the timescale of the spin dynamics.

In the following, we assume that the characteristic frequency ν_1 depends on temperature according to an Arrhenius law,

$$\nu_1(T) = \nu_0 e^{-B/T}, \quad (4)$$

where B is a typical energy barrier for rearrangements. This choice takes into account, at a qualitative level, the thermally activated nature of rearrangements, thereby inducing at low temperature T a timescale separation between the fast spin dynamics and the slow coupling dynamics.

It is important to note that the slowdown of the relaxation time of the spin dynamics does not result from the Arrhenius form of the timescale $\tau_1 = 1/\nu_1$ defined in Eq. (4), but rather from the spin dynamics itself that slows when lowering temperature, due to interactions between spins. If one would freeze the disordered couplings (i.e., $\nu_1 = 0$) and thus consider a spin-glass model, the relaxation time would also increase when lowering temperature, and eventually diverge when $T \rightarrow 0$. Hence the role of the phenomenological activated frequency ν_1 introduced in Eq. (4) is to provide a mechanism for the unfreezing of the disorder on long timescale, to recover effectively noninteracting spins at equilibrium (i.e., in the infinite time limit), consistently with experimental results. In the following, we use in numerical simulations the value $B = 3J_0$, which ensures that rearrangements are slow enough to let the glassy dynamics unfold, but fast enough to see a decorrelation at low frequency in the nonlinear response (see Sec. IV).

B. Kinetically constrained model

We wish to compare the above model of interacting spins with stochastic couplings to a simple kinetically constrained model (KCM). As a minimal KCM, we consider a simple extension of the Fredrickson-Andersen (FA) model [19] that includes spin variables on top of the usual mobility excitations. KCM with two local variables have been previously considered in other contexts, like ion mobility in glasses [53]. In the usual FA model, mobility excitations are the only

degrees of freedom (so that kinetic constraints only affect mobility excitations themselves), while in our model mobility excitations may couple to other physical degrees of freedom. More explicitly, we introduce local facilitation variables $n_i = 0$ or 1 on each site i , where $n_i = 1$ corresponds to the presence of a mobility excitation on site i . As in the FA model, mobility excitations are assumed to be noninteracting, and thus to contribute to the Hamiltonian through a term proportional to $\sum_i n_i$. The generalized Hamiltonian then reads

$$\tilde{H} = -E(t) \sum_{i=1}^N S_i + K \sum_{i=1}^N n_i, \quad (5)$$

with the external field $E(t)$ and a characteristic energy K of mobility excitations. A spin S_i can be flipped only when $n_i = 1$, which leads to a slowdown of the dynamics at low temperature, because mobility excitations become rare due to their energetic cost. The transition rate for spin reversal reads

$$W(-S_i|S_i) = \frac{v_0 n_i}{1 + e^{\beta \Delta \tilde{H}_i^S}}, \quad (6)$$

where $\Delta \tilde{H}_i^S = 2ES_i$ is the variation of the Hamiltonian \tilde{H} defined in Eq. (5) associated with the transition $S_i \rightarrow -S_i$. Here again, we assume the transition rates to be slowly time-dependent due to the field $E(t)$. As for the dynamics of mobility excitations, we follow the standard rules of the FA model. The local variable n_i can change its value only if at least one of the neighboring variables n_{i-1} or n_{i+1} is equal to 1 . On a coarse-grained scale, this kinetic constraint on the dynamics of the variables n_i leads to an effective diffusion of mobility excitations [19]. To fulfill detailed balance with respect to the Hamiltonian (5), and to take into account kinetic constraints on the dynamics of mobility excitations, we choose the following form for the transition rate from n_i to $n'_i = 1 - n_i$:

$$W(1 - n_i|n_i) = \frac{v_0}{1 + e^{\beta \Delta \tilde{H}_i^n}} \theta(n_{i-1} + n_{i+1}), \quad (7)$$

where $\theta(x)$ is the Heaviside function, $\theta(x) = 1$ if $x > 0$ and $\theta(x) = 0$ otherwise; $\Delta \tilde{H}_i^n = K(1 - 2n_i)$ is the variation of the Hamiltonian \tilde{H} defined in Eq. (5) associated with the transition $n_i \rightarrow 1 - n_i$.

III. STATIC THIRD-ORDER RESPONSE

A. General expression of cubic responses

We first consider a generic spin model at equilibrium, with a Hamiltonian H , which is a function of N spin variables $\{S_i\}$ and possibly of other variables present in the system. Spins are coupled to a static external field E_0 , so that the Hamiltonian takes the form

$$H = H_0 - E_0 \sum_i S_i, \quad (8)$$

where H_0 is the Hamiltonian in the absence of external field ($E_0 = 0$). We assume that H_0 is invariant by global spin reversal $\{S_i\} \rightarrow \{-S_i\}$. The free energy density is defined by

$$f = -\frac{1}{\beta N} \ln Z, \quad (9)$$

where $Z = \sum_{\mathcal{C}} e^{-\beta H(\mathcal{C})}$ is the partition function; \mathcal{C} is a short-hand notation for the list of all microscopic variables, including the N spins S_i . The average magnetization $\langle m \rangle$, where $m = \frac{1}{N} \sum_{i=1}^N S_i$, is given by

$$\langle m \rangle = -\frac{\partial f}{\partial E_0}. \quad (10)$$

Static linear and nonlinear responses are obtained by expanding $\langle m \rangle$ for small E_0 ,

$$\langle m \rangle = \chi_1^s E_0 + \chi_3^s E_0^3 + \dots, \quad (11)$$

where we have kept terms only up to third order, and used the spin-reversal symmetry to eliminate even terms in E_0 in the expansion. This leads in particular to a definition of a static cubic response as

$$\chi_3^s = \frac{1}{6} \frac{\partial^3 \langle m \rangle}{\partial E_0^3}. \quad (12)$$

An alternative expression of the cubic response is obtained by considering a field $E_0 + \varepsilon$ and evaluating the linear response to the tiny contribution $\varepsilon \ll E_0$, in the presence of the small field E_0 . Here one considers the linear response

$$\chi_{\text{lin}}^s(E_0) = \frac{\partial \langle m \rangle}{\partial E_0} \quad (13)$$

and expands it to quadratic order in E_0 ,

$$\chi_{\text{lin}}^s(E_0) = \chi_1^s + \chi_{21}^s E_0^2 + \dots, \quad (14)$$

which defines the cubic response χ_{21}^s . Using Eqs. (11) and (13), we obtain

$$\chi_{\text{lin}}^s = \chi_1^s + 3\chi_3^s E_0^2 + \dots \quad (15)$$

One thus has the simple relation between the cubic responses χ_3^s and χ_{21}^s :

$$\chi_{21}^s = 3\chi_3^s. \quad (16)$$

As we will see below in Sec. IV, the static response χ_{21}^s corresponds to the zero-frequency limit of the dynamic cubic response considered in this paper, and we thus focus on χ_{21}^s rather than on χ_3^s in the following.

From Eqs. (12) and (16) we have

$$\chi_{21}^s = \frac{1}{2} \frac{\partial^3 \langle m \rangle}{\partial E_0^3}. \quad (17)$$

Using Eq. (10), we eventually end up with

$$\chi_{21}^s = -\frac{1}{2} \frac{\partial^4 f}{\partial E_0^4}. \quad (18)$$

This general expression of the static third-order response χ_{21}^s can now be applied to the two spin models introduced in Sec. II.

B. Spin model with stochastic couplings

We consider the spin model with stochastic couplings defined in Sec. II A, with a static external field $E(t) = E_0$. Using the expression (1) of the Hamiltonian H , the partition function

reads

$$Z = \sum_{\{S_i\}, \{J_{i,i+1}\}} e^{\beta \sum_{i=1}^N J_{i,i+1} S_i S_{i+1} + \beta E_0 \sum_{i=1}^N S_i}, \quad (19)$$

and it can be determined for instance using a standard transfer matrix technique. However, a simpler calculation can be performed using a change of summation variable. Defining $\sigma_i = J_{i,i+1} S_i S_{i+1} / J_0$, the partition function takes the simpler form

$$Z = \sum_{\{S_i\}, \{\sigma_i\}} e^{\beta J_0 \sum_{i=1}^N \sigma_i + \beta E_0 \sum_{i=1}^N S_i}, \quad (20)$$

which now effectively involves only noninteracting degrees of freedom (the sum is performed over all values $S_i = \pm 1$ and $\sigma_i = \pm 1$ for $i = 1, \dots, N$). One thus finds

$$Z = [4(\cosh \beta J_0) \cosh(\beta E_0)]^N. \quad (21)$$

The free energy density defined in Eq. (9) then reads

$$f(\beta, E_0) = f_{\text{int}}(\beta) + f_{\text{id}}(\beta, E_0), \quad (22)$$

where

$$f_{\text{int}}(\beta) = -\frac{1}{\beta} \ln[2 \cosh(\beta J_0)] \quad (23)$$

is the contribution to the free energy density resulting from (annealed) random interactions between spins, and

$$f_{\text{id}}(\beta, E_0) = -\frac{1}{\beta} \ln[2 \cosh(\beta E_0)] \quad (24)$$

is the free energy density of the ideal spin gas. Hence at static level, interactions between spins are decoupled from the external field, in the sense that their respective contribution to the free energy density is additive. Equations (10), (11), and (18) then lead to simple expressions for the static linear and third-order responses, respectively,

$$\chi_1^s = \beta, \quad \chi_{21}^s = -\beta^3, \quad (25)$$

which are nothing but the linear and third-order responses of an ideal spin gas, i.e., a paramagnetic system of noninteracting spins. The linear response exhibits a moderate increase, $\propto 1/T$, when lowering temperature, in qualitative agreement with experiments. Note that only $f_{\text{id}}(\beta, E_0)$ contributes to the response χ_{21}^s , because only this contribution to the free energy density depends on the field E_0 .

C. Kinetically constrained spin model

For the kinetically constrained spin model introduced in Sec. II B, considered here with a static field $E(t) = E_0$, the partition function defined by the Hamiltonian \tilde{H} given in Eq. (5) reads as

$$Z_{\text{kc}} = \sum_{\{S_i\}, \{n_i\}} e^{\beta E_0 \sum_{i=1}^N S_i - \beta K \sum_{i=1}^N n_i}. \quad (26)$$

The spins S_i and mobility excitations n_i are noninteracting variables in the Hamiltonian \tilde{H} , so that the partition function simply factorizes as

$$Z_{\text{kc}} = [4(\cosh \beta K) \cosh(\beta E_0)]^N. \quad (27)$$

The free energy density again takes an additive form

$$f_{\text{kc}}(\beta, E_0) = f_{\text{mob}}(\beta) + f_{\text{id}}(\beta, E_0), \quad (28)$$

where

$$f_{\text{mob}}(\beta) = -\frac{1}{\beta} \ln[2 \cosh(\beta K)] \quad (29)$$

is the free energy contribution of mobility excitations, and where the ideal spin gas contribution $f_{\text{id}}(\beta, E_0)$ has the same expression as in Eq. (24). Hence, one also finds for the kinetically constrained model that the linear and third-order static responses are given by the ideal spin gas responses $\chi_1^s = \beta$ and $\chi_{21}^s = -\beta^3$, respectively, as in Eq. (25). Note that this result was expected since spins are noninteracting in the present model.

IV. DYNAMIC THIRD-ORDER RESPONSE

Our goal is to evaluate the third-order (dielectric) response of the polarization (i.e., magnetization in the spin language) to a time-dependent external field $E(t)$ oscillating at (angular) frequency ω . Here again, there are several ways to define a third-order response. For instance, one may consider either the response to the field at frequency ω or at frequency 3ω . The response at frequency ω can itself be divided into two distinct response functions. As in the static case, we focus here on the simplest third-order response function, called $\chi_{21}(\omega)$, which consists in looking at the third-order response at frequency ω when applying a field $E(t) = E_0 + \varepsilon \cos(\omega t)$, in the limit where both the static component E_0 and the amplitude ε are small, with the further assumption that $\varepsilon \ll E_0$. The third-order response $\chi_{21}(\omega)$, which has been measured experimentally [54], is linear in ε and quadratic in E_0 , yielding an overall third-order response in the field amplitude. It has been shown that all types of third-order responses behave in a similar way [38,54], and it is thus legitimate to focus on a specific type of response.

A. Fluctuation-dissipation relation

The advantage of the third-order response function $\chi_{21}(\omega)$ is that it consists in a linear response to the oscillating contribution of the field. In other words, it is the correction at order E_0^2 to the linear response $\chi(\omega, E_0)$ of the polarization at frequency ω ,

$$\chi_{21}(\omega) = \frac{1}{2} \frac{\partial^2 \chi}{\partial E_0^2}(\omega, E_0 = 0). \quad (30)$$

Interestingly, the linear response $\chi(\omega, E_0)$ in the presence of a static field E_0 can be expressed in terms of the equilibrium correlation function of the magnetization using the fluctuation-dissipation theorem (FDT) since we are dealing with a close-to-equilibrium situation. We first formulate the FDT in the time domain before moving to the frequency domain. Let us define the (normalized) equilibrium two-time correlation function of the magnetization, $m(t) = N^{-1} \sum_{i=1}^N S_i(t)$, as

$$C(t, E_0) = N(\langle m(t)m(0) \rangle_{E_0} - \langle m \rangle_{E_0}^2), \quad (31)$$

where the notation $\langle \cdots \rangle_{E_0}$ indicates an average over the equilibrium dynamics under a static field E_0 . The FDT then reads

$$\chi(t, E_0) = -\beta\theta(t) \frac{\partial C}{\partial t}(t, E_0), \quad (32)$$

where $\chi(t, E_0)$ is the impulse response [i.e., the linear response of $\langle m(t) \rangle_{E_0}$ to a Dirac delta in $\varepsilon(t)$ for a field $E(t) = E_0 + \varepsilon(t)$], and $\theta(t)$ is the Heaviside function which accounts for the causality condition.

In practice, we may thus use the following procedure to determine numerically the third-order response $\chi_{21}(\omega)$. One first determines the equilibrium spin correlation function $C(t, E_0)$ in the time domain for different small values of the static field E_0 , and then take its Fourier-Laplace transform $\hat{C}(\omega, E_0)$, defined as

$$\hat{C}(\omega, E_0) = \int_0^\infty dt e^{i\omega t} C(t, E_0). \quad (33)$$

In Fourier space, the FDT (32) reads

$$\chi(\omega, E_0) = \beta C(t=0, E_0) + \beta i\omega \hat{C}(\omega, E_0). \quad (34)$$

Note that we consider here both the real and imaginary parts of the Fourier transform of the fluctuation-dissipation relation (32), while standard forms of the fluctuation-dissipation relation in Fourier space usually include only the imaginary part of Eq. (34), corresponding to the loss modulus.

Setting $E_0 = 0$ in Eq. (34), one gets the linear response function $\chi_1(\omega)$,

$$\chi_1(\omega) = \beta C(0, 0) + \beta i\omega \hat{C}(\omega, 0). \quad (35)$$

The third-order response function $\chi_{21}(\omega)$ is obtained by applying the definition (30) to the fluctuation-dissipation relation (34), yielding

$$\chi_{21}(\omega) = \frac{\beta}{2} \frac{\partial^2 C}{\partial E_0^2}(0, 0) + \frac{1}{2} \beta i\omega \frac{\partial^2 \hat{C}}{\partial E_0^2}(\omega, 0). \quad (36)$$

Note that in practice, one needs to determine numerically the correlation function with high accuracy in order to evaluate the second derivative of the correlation function with respect to E_0 . An advantage of the method described here is that only static fields are applied in the simulations.

B. Spin model with stochastic couplings

We have determined numerically both the linear and the third-order response functions $\chi_1(\omega)$ and $\chi_{21}(\omega)$ using kinetic Monte Carlo simulations of the spin model defined by Eqs. (1), (2), and (3). To obtain the frequency-dependent response functions $\chi_1(\omega)$ and $\chi_{21}(\omega)$ over a broad range of frequencies, we first perform accurate fits of the time-dependent correlation function $C(t, E_0)$ for $E_0 = 0$ and for a small, nonzero value E_0 . Fits of $C(t, E_0)$ are constrained to take the known equilibrium value

$$C(0, E_0) = N(\langle m^2 \rangle_{E_0} - \langle m \rangle_{E_0}^2), \quad (37)$$

which is computed from the second derivative of the free energy (22) with respect to the field. The linear response function is evaluated from $C(t, 0)$ using Eq. (35). The third-order

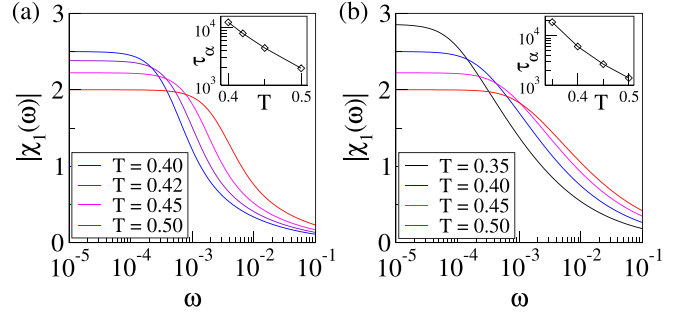


FIG. 1. Modulus of the linear response $\chi_1(\omega)$ as a function of the angular frequency ω , for different values of temperature (same color code on both panels). (a) Spin model with stochastic couplings for $T = 0.40, 0.42, 0.45, 0.50$, from top to bottom at low ω ($J_0 = 1, B = 3$). Inset: relaxation time $\tau_\alpha = 2\pi/\omega_\alpha$ vs temperature T , where ω_α is the angular frequency at which the imaginary part $\chi_1''(\omega)$ is maximum. (b) Kinetically constrained spin model for $T = 0.35, 0.40, 0.45, 0.50$, from top to bottom at low ω ($K = 1$). Inset: τ_α vs T . In both cases, the response function decays monotonously with frequency. System size: $N = 10^3$ for (a) and (b).

response is obtained from Eq. (36), using the approximation

$$\frac{\partial^2 C}{\partial E_0^2}(t, 0) \approx \frac{2}{E_0^2} [C(t, E_0) - C(t, 0)], \quad (38)$$

which holds since $C(t, E_0)$ is an even function of E_0 . The modulus $|\chi_1(\omega)|$ of the linear response is plotted in Fig. 1(a) for several temperature values. The modulus $|\chi_{21}(\omega)|$ of the third-order response is plotted in Fig. 2 for different values of the temperature T (we set $k_B = 1$). At a qualitative level, the response function is seen to have the typical humped shape reported in experiments.

Simulations have been performed using a moderate system size $N = 10^3$, and averaging over 10^5 independent runs, to get

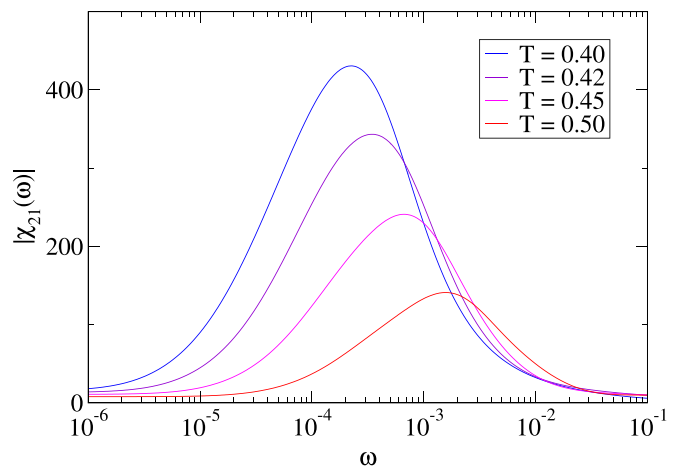


FIG. 2. Modulus of the third-order response $\chi_{21}(\omega)$ for different values of temperature ($T = 0.40, 0.42, 0.45, 0.50$, from top to bottom) in the spin model with stochastic couplings, exhibiting a pronounced peak whose height increases when decreasing temperature, while peak frequency decreases with temperature. Parameters: $J_0 = 1, B = 3, N = 10^3$. The third-order response is obtained from the time correlation $C(t, E_0) - C(t, 0)$ evaluated for $E_0 = 0.04$.

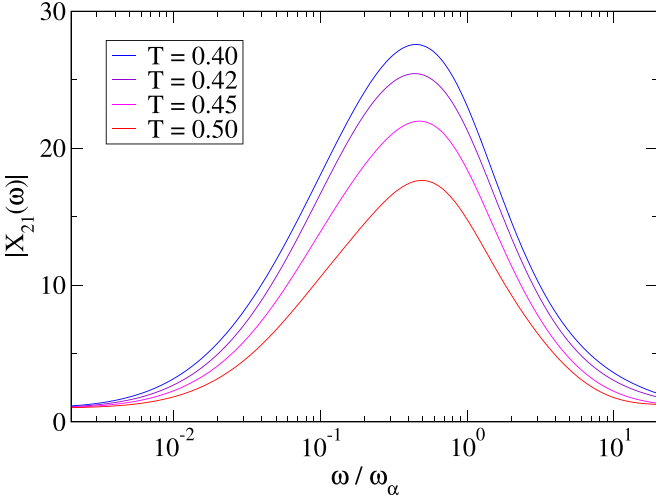


FIG. 3. Modulus $|X_{21}(\omega)|$ of the rescaled third-order response in the spin model with stochastic couplings, as a function of the rescaled frequency $\omega/\omega_\alpha(T)$, for different values of temperature ($T = 0.40, 0.42, 0.45, 0.50$, from top to bottom; same data as Fig. 2). The peak value increases when decreasing temperature.

accurate data. This procedure has been found to yield cleaner data than simulations of a larger system averaged over a lower number of runs. We checked that the system size considered remains much larger than the rigidity length (see Sec. V).

To investigate the effect of temperature, we define a rescaled third-order response $X_{21}(\omega) = T^3 \chi_{21}(\omega)$ that normalizes the response $\chi_{21}(\omega)$ by the static third-order response of noninteracting dipoles, which is equal to $1/T^3$ in the present model [see Eq. (25)] –or proportional to $1/T^3$ in experiments. Any temperature dependence of the curve $X_{21}(\omega)$ is thus expected to be due to interactions. We have plotted $X_{21}(\omega)$ in Fig. 3 as a function of the rescaled frequency $\omega/\omega_\alpha(T)$, where $\omega_\alpha(T)$ is the value of ω for which the loss modulus $\chi_1''(\omega)$, that is, the imaginary part of the linear response function, is maximal ($\tau_\alpha = 2\pi/\omega_\alpha$ is the relaxation time). We observe that in this rescaled representation, the peak value still increases when decreasing temperature, in qualitative agreement with experimental results [28]. Note that to obtain these results, one needs to take into account an increased timescale separation between spin and coupling dynamics when temperature is lowered, as accounted for by the Arrhenius law in Eq. (4).

C. Kinetically constrained spin model

We have also evaluated the dynamic linear and cubic responses $\chi_1(\omega)$ and $\chi_{21}(\omega)$ in the kinetically constrained spin model defined in Sec. II B. The same fitting protocol as the one described in Sec. IV B is used. The modulus $|\chi_1(\omega)|$ of the linear response is plotted in Fig. 1(b) and is observed to monotonously decrease with frequency as expected. The modulus $|\chi_{21}(\omega)|$ of the cubic response is plotted in Fig. 4. We see that contrary to the model of interacting spins, no peak is observed and $|\chi_{21}(\omega)|$ decreases monotonically as a function of the frequency ω . The curves approximately collapse to a master curve when rescaled by $1/T^3$, up to a simultaneous rescaling of frequency into $\omega/\omega_\alpha(T)$. The corresponding plot

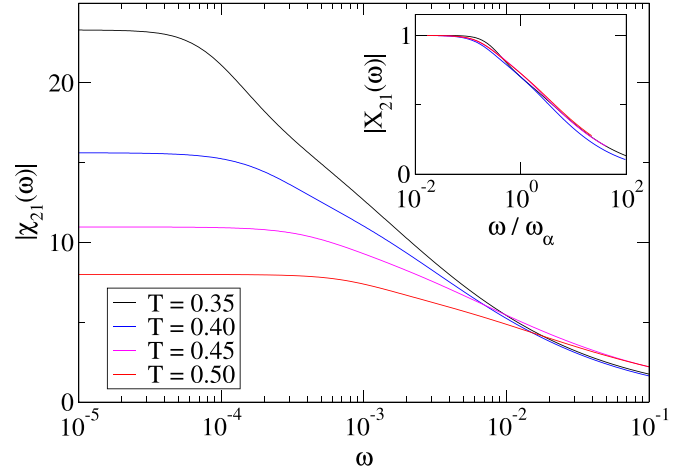


FIG. 4. Modulus $|\chi_{21}(\omega)|$ of the third-order response for different values of temperature ($T = 0.35, 0.40, 0.45, 0.50$, from top to bottom) in the kinetically constrained spin model. No peak is observed, and $|\chi_{21}(\omega)|$ decreases monotonically with frequency. Inset: corresponding rescaled response $|X_{21}(\omega)|$ vs rescaled frequency $\omega/\omega_\alpha(T)$. Parameters: $K = 1, N = 10^3$. The third-order response is obtained from $C(t, E_0) - C(t, 0)$ evaluated for $E_0 = 0.13, 0.15, 0.18, 0.20$ at temperature $T = 0.35, 0.40, 0.45, 0.50$, respectively.

of the rescaled response $|X_{21}(\omega)| = T^3 |\chi_{21}(\omega)|$ vs $\omega/\omega_\alpha(T)$ is displayed in the inset of Fig. 4.

Summarizing Sec. IV, we have found that the two models studied have the same behavior for the linear response $|\chi_1(\omega)|$, but differ considerably in the shape of $|\chi_{21}(\omega)|$, although they have the same trivial static responses $\chi_1(0)$ and $\chi_{21}(0)$. At a qualitative level, only the model with slowly rearranging, spin-glass-like couplings is consistent with the experimental behavior reported in supercooled liquids. This shows in particular that a model with local facilitation as the only physical ingredient fails to reproduce the peaked shape of the third-order response. In the next section we look for a scenario capturing more in depth the source of this difference between the two models.

V. A TWO-LENGTH-SCALE SCENARIO

As explained in the Introduction, nonlinear dielectric responses are mostly used as experimental tools to probe the presence of a dynamic length ℓ_{NonLin} in glass formers. Numerically, more direct measures of dynamical length can be performed. We argue below in favor of a two-length scale scenario in the dynamics of the glassy spin model with stochastic couplings. This scenario allows us to evidence the key role played by interactions to generate a dynamic rigidity length that becomes significantly larger than the dynamic length scale characterizing dynamical heterogeneities. We start by recalling the heuristic “superdipole” argument, which is useful to grasp the physical picture behind the humped shape of the cubic response.

A. Superdipole picture

1. Physical motivation

Obtaining the humped shape of the cubic response is non-trivial in the sense that it requires two important ingredients

of the model, namely, the presence of interactions between spins and the timescale separation between the dynamics of the spins and that of the couplings. In the absence of interactions ($J_0 = 0$), the model reduces to a paramagnetic spin model (or ideal spin gas) also in the dynamical regime, and $|\chi_{21}(\omega)|$ is expected to be a decreasing function of ω , with a low-frequency plateau value equal to $1/T^3$, in agreement with the static results of Sec. III [see Eq. (25)]. Including interactions with nonzero quenched couplings $J_{i,i+1}$ leads to the emergence of a rigidity length, that grows when decreasing temperature, as discussed below.

Heuristically, and as long as the frequency is not too low, the system may be thought of as an ideal gas of superdipoles, as mentioned above, where superdipoles are composed of typically $N_{\text{corr}}(T)$ neighboring spins with an essentially frozen disordered structure. Hence $\chi_{21}(\omega)$ is expected to remain a decreasing function of ω , but now with a higher low-frequency plateau value (see below). To get the humped shape, one thus needs to take into account the slow dynamics of the coupling constants, on a timescale much larger than the one of the spin dynamics. In this low-frequency regime, the third-order response thus goes from the high plateau value $\propto N_{\text{corr}}(T)/T^3$ down to the ideal gas nonlinear response equal to $1/T^3$.

In its simplest version, the superdipole argument assumes that the N spins can be divided into groups of N_{corr} neighboring spins that flip simultaneously, and thus constitute a superdipole (or “superspin”). Interactions between superdipoles are neglected. To formulate the argument in a quantitative way, it is thus useful to first evaluate the dynamic response of noninteracting spins.

2. Dynamic response of noninteracting spins

For later generalization to the superdipole case, it is convenient to assume that the spins take values $S_i = \pm\mu$, where μ is the dipolar moment. The transition rate for spin reversal is given by

$$W(-S_i|S_i) = \frac{\nu_0}{1 + e^{2\beta\mu E S_i}}. \quad (39)$$

For noninteracting spins, the dynamic response can be evaluated from the study of a single spin S (where S is any of the spins S_i). Due to the absence of (both static and dynamic) correlations between different spins, the equilibrium magnetization correlation $C(t, E)$ defined in Eq. (31) boils down to the single-spin two-time correlation

$$C_S(t, E_0) = \langle S(t)S(0) \rangle_{E_0} - \langle S \rangle_{E_0}^2. \quad (40)$$

For the two-state stochastic process defined by the transition rate (39), the time-dependent solution of the master equation can be written explicitly. The correlation $C_S(t, E)$ is obtained as

$$C_S(t, E) = \mu^2 [1 - \tanh^2(\beta\mu E)] e^{-\nu_0 t}. \quad (41)$$

One then obtains from Eqs. (33) and (34),

$$\chi(\omega, E) = \frac{\mu^2 \beta}{1 - i\omega\tau} [1 - \tanh^2(\beta\mu E)], \quad (42)$$

with $\tau = \nu_0^{-1}$. This respectively leads for the linear and cubic responses to

$$\chi_1(\omega) = \frac{\mu^2 \beta}{1 - i\omega\tau}, \quad \chi_{21}(\omega) = -\frac{\mu^4 \beta^3}{1 - i\omega\tau}. \quad (43)$$

Static results of Sec. III are recovered in the limit $\omega \rightarrow 0$, for $\mu = 1$. The moduli of the linear and cubic responses are decreasing functions of the frequency,

$$|\chi_1(\omega)| = \frac{\mu^2 \beta}{\sqrt{1 + (\omega\tau)^2}}, \quad |\chi_{21}(\omega)| = \frac{\mu^4 \beta^3}{\sqrt{1 + (\omega\tau)^2}}. \quad (44)$$

Expanding more generally $\chi(\omega, E)$ in powers of E ,

$$\chi(\omega, E) = \sum_{n=0}^{\infty} \chi_{2n,1}(\omega) E^{2n} \quad (45)$$

with $\chi_{0,1} \equiv \chi_1$, one finds in the same way that

$$|\chi_{2n,1}(\omega)| \propto \frac{\mu^{2+2n} \beta^{1+2n}}{\sqrt{1 + (\omega\tau)^2}} \quad (46)$$

is a decreasing function of ω .

3. Dynamic response of noninteracting superdipoles

In the superdipole picture, one assumes that interactions make spins move coherently as blocks of N_{corr} spins. Yet each block of spin has a disordered internal structure due to the glassy nature of the system. One is thus led to consider superdipoles with a dielectric moment $\mu \approx N_{\text{corr}}^{1/2} \mu_0$, with μ_0 the individual dielectric moment. Since the dynamic response is evaluated as a density with respect to the number of spins (and not of superdipoles), it has to be further normalized by N_{corr} . One ends up with

$$|\chi_{2n,1}^{\text{sd}}(\omega)| \propto \frac{(\sqrt{N_{\text{corr}}} \mu_0)^{2+2n} \beta^{1+2n}}{N_{\text{corr}} \sqrt{1 + (\omega\tau)^2}} \propto \frac{N_{\text{corr}}^n}{\sqrt{1 + (\omega\tau)^2}}, \quad (47)$$

where the superscript “sd” stands for “superdipoles.” The experimentally observed humped shape of the third and fifth order nonlinear responses suggests that at very low frequency, N_{corr} should actually be an increasing function of ω , that saturates to a finite value at higher frequencies. This is consistent with the fact that correlations are weak or even absent at equilibrium. Assuming a slow enough increase of $N_{\text{corr}}(\omega)$, the above calculation still approximately applies, and one finds

$$|\chi_{2n,1}^{\text{sd}}(\omega)| \propto \frac{N_{\text{corr}}(\omega)^n}{\sqrt{1 + (\omega\tau)^2}}, \quad (48)$$

which reproduces the typical humped shape of nonlinear responses. Consistently with experiments, one finds that the linear response is independent of N_{corr} , and that for large N_{corr} , the nonlinear responses become larger when their order $2n + 1$ is increased.

The spin models considered in this work offer an interesting opportunity to assess and substantiate the superdipole picture. The latter assumes that blocks of spins move coherently, which can be interpreted as a local rigidity of the spin dynamics. We introduce below a tool to characterize the local rigidity of the spin dynamics, and we apply it to both the interacting spin model with slowly rearranging couplings introduced in Sec. II A, and to the KCM defined in Sec. II B.

B. Dynamical rigidity length

In order to assess the validity of the superdipole picture, we need to test whether spins effectively move as rigid blocks, whose size needs to be determined. This task is complicated by the fact that the spin structure is disordered, and no spatial order is visible. To test the superdipole hypothesis whereby spins flip as rigid blocks, we need to check whether, in a given time window, spins separated by a distance r have flipped the same number of times. However, note that the superdipole assumption may be too stringent. In practice, spins in our model move one by one, but may tend on a coarse-grained timescale to behave as spin blocks, or superdipoles. In particular, spins may at some point flip randomly, and swiftly flip back to the block configuration (which we interpret below as the presence of restoring forces; see Sec. VI A 2). Such short excursions out of the block behavior change the number of flips with respect to the pure superdipole behavior, but mostly do not change the parity of the number of flips. With this aim in mind, we introduce the local overlap variable $q_i(t) = S_i(t)S_i(0)$ between the values of spin S_i at $t = 0$ and t . The local overlap $q_i(t)$ measures the parity of the number of flips in the time interval $[0, t]$. Hence, in spite of the presence of a disordered spin structure, the overlaps $q_i(t)$ and $q_{i+r}(t)$ have the same value if spins S_i and S_{i+r} flip simultaneously, as in the superdipole picture where blocks of spins simultaneously flip. They keep the same parity if only short excursions occur, as discussed above. In contrast, if the flips of spins S_i and S_{i+r} are not strongly correlated, the values of the overlaps $q_i(t)$ and $q_{i+r}(t)$ tend to decorrelate after the first flips. The spatial correlation of the local overlap variables $q_i(t)$ and $q_{i+r}(t)$ is thus a way to determine the size of spin domains which effectively move as a block, which is equivalent to the superdipole size N_{corr} in the present one-dimensional setting. Therefore, we define the four-point correlation $g_4^q(r, t)$ as the spatial correlation of the two-time local overlap variable $q_i(t)$:

$$g_4^q(r, t) = \langle \langle q_i(t)q_{i+r}(t) \rangle_i - \langle q_i(t) \rangle_i \langle q_{i+r}(t) \rangle_i \rangle_{\text{tr}}, \quad (49)$$

where $\langle \dots \rangle_i$ denotes a spatial average over site i , and $\langle \dots \rangle_{\text{tr}}$ stands for an ensemble average over stochastic trajectories and initial conditions. The associated four-point susceptibility $\chi_4^q(t)$ then reads

$$\chi_4^q(t) = \sum_r g_4^q(r, t). \quad (50)$$

In the present one-dimensional context, we define a rigidity length ξ_{rig} by normalizing $\chi_4^q(t)$ by $g_4^q(0, t)$ as

$$\xi_{\text{rig}}(t) = \frac{\chi_4^q(t)}{g_4^q(0, t)}. \quad (51)$$

As discussed above, the length $\xi_{\text{rig}}(t)$ characterizes how, on a timescale t , spins effectively move as blocks of size $\xi_{\text{rig}}(t)$. We call it the ‘‘dynamical rigidity length’’ $\xi_{\text{rig}}(t)$ rather than N_{corr} first to emphasize that it is a length, but also to outline its interpretation in terms of a local rigidity of the dynamics, an idea which is less clearly conveyed by the term ‘‘correlated volume’’ associated with N_{corr} .

C. Dynamical heterogeneities

We now aim at determining a correlation length ξ_{dh} of dynamical heterogeneities that can be quantitatively compared to the rigidity length ξ_{rig} . Here we do not want to characterize the potential rigidity of the spin dynamics, but rather the fact that over a given time window $[0, t]$, some spatial domains have relaxed while others have not moved. The characteristic size of these domains is the dynamical heterogeneity length ξ_{dh} . Dynamical heterogeneities in spin models can be characterized by introducing a local persistence variable $\phi_i(t)$ that satisfies $\phi_i(0) = 1$ and keeps the value $\phi_i(t) = 1$ as long as the spin S_i does not flip. A standard choice is then to assign the value 0 to the persistence variable after the first spin flip, whatever the later spin value (see, e.g., [55,56]). Here, to remain as close as possible to the overlap variable $q_i(t)$ defined in Sec. VB, we instead assume that at each flip of spin S_i , $\phi_i(t)$ is randomly assigned a value ± 1 , with equal probability. In this way, $\phi_i(t)$ takes values ± 1 similarly to $q_i(t)$, but correlations with the value $S_i(0)$ are lost after the first spin flip. The randomization of the sign of $\phi_i(t)$ after the first flip precisely gets rid of the information on the rigidity or not of the dynamics, so as to focus on the spatially heterogeneous character of the relaxation dynamics.

We define the four-point correlation function $g_4^\phi(r, t)$ as the spatial correlation function of the two-time variables $\phi_i(t)$,

$$g_4^\phi(r, t) = \langle \langle \phi_i(t)\phi_{i+r}(t) \rangle_i - \langle \phi_i(t) \rangle_i \langle \phi_{i+r}(t) \rangle_i \rangle_{\text{tr}}, \quad (52)$$

with the same notations for averages as in Eq. (49). The corresponding four-point susceptibility $\chi_4^\phi(t)$ reads as

$$\chi_4^\phi(t) = \sum_r g_4^\phi(r, t). \quad (53)$$

The correlation length ξ_{dh} characterizing dynamical heterogeneities is then defined by normalizing $\chi_4^\phi(t)$ by $g_4^\phi(0, t)$ as

$$\xi_{\text{dh}}(t) = \frac{\chi_4^\phi(t)}{g_4^\phi(0, t)}. \quad (54)$$

D. Numerical results

1. Spin model with stochastic couplings

We have evaluated numerically the correlation lengths $\xi_{\text{rig}}(t)$ and $\xi_{\text{dh}}(t)$ in the spin model with random couplings defined in Sec. II A. These two length scales are plotted in Fig. 5 for different values of temperature T .

Lowering temperature, the timescale separation between spin dynamics and coupling dynamics is increased, i.e., $\nu_1(T)/\nu_0 \ll 1$. In this regime, the rigidity length $\xi_{\text{rig}}(t)$ becomes much larger than the characteristic length $\xi_{\text{dh}}(t)$ of dynamical heterogeneities for times $t \gtrsim \tau_\alpha$, and its maximum shifts to larger times with respect to that of $\xi_{\text{dh}}(t)$. We note in particular that $\xi_{\text{rig}}(t)$ still takes appreciable values in a time regime when $\xi_{\text{dh}}(t)$ has already relaxed to a value close to unity. These results indicate that after their first flip, spins continue to effectively move as spin blocks of size $\sim \xi_{\text{rig}}$ over an appreciable time window, until these blocks eventually melt, and rigidity is lost. This transient rigidity

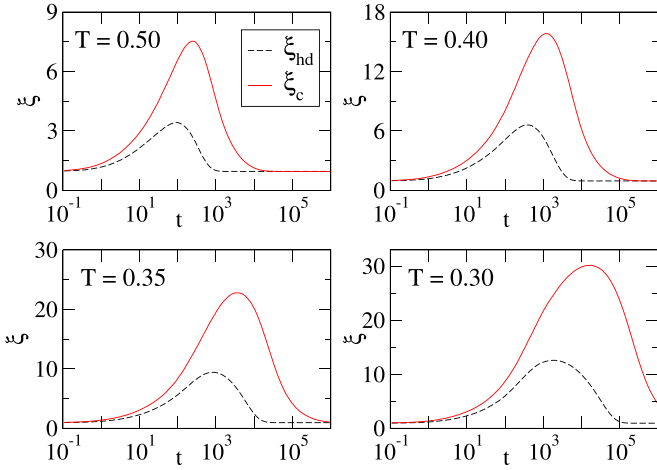


FIG. 5. Dynamic lengths ξ_{dh} characterizing dynamical heterogeneities (dashed line) and ξ_{rig} characterizing cooperative effects (full line) as a function of time t in the spin model with stochastic couplings, for different values of temperature T . Note that the Y -axis scale changes from one panel to the other to enhance readability. At low temperature, $\xi_{rig}(t)$ becomes much larger than $\xi_{dh}(t)$ for $t \gtrsim \tau_\alpha$, showing that interactions play the role of a restoring force (see Sec. VIA 2) when couplings change very slowly. Parameters: $J_0 = 1, B = 3, N = 10^3$.

precisely results from the presence of interactions between spins, which yield a preferred disordered configuration of the block (up to a flip of the block). The rigidity length $\xi_{rig}(t)$ originates from the spin-glass correlation length that would develop under the effect of quenched disorder, but can only partially unfold due to the slow rearrangements of the coupling constants.

2. Kinetically constrained spin model

To compare these results with the basic facilitation picture, we plot in Fig. 6 the characteristic lengths $\xi_{rig}(t)$ and $\xi_{dh}(t)$ for the KCM defined in Sec. II B, for different temperature values. We observe that in this case ξ_{rig} remains almost identical to ξ_{dh} , meaning that glassy relaxation is dominated here

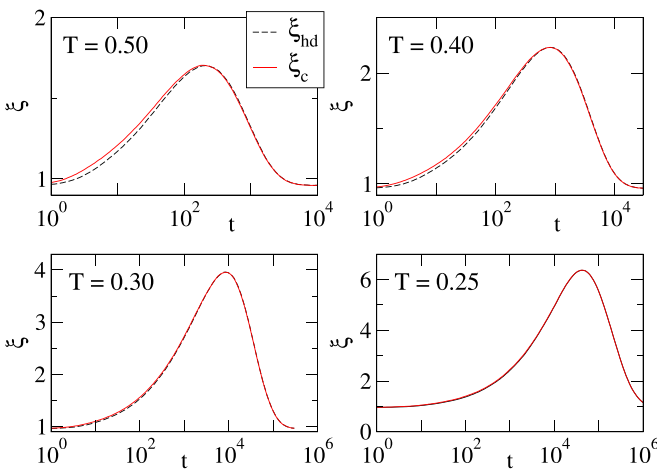


FIG. 6. Dynamic lengths ξ_{dh} (dashed line) and ξ_{rig} (full line) as a function of time t in the kinetically constrained spin model, for different values of temperature T . Parameters: $K = 1, N = 10^3$.

by dynamical heterogeneities. This means that no dynamical rigidity is present in the model, consistent with the fact that spins are noninteracting. Even though spins might seemingly move as blocks due to dynamical heterogeneities, rigidity is essentially lost after a flip as no interactions are present to select a preferred disordered configuration whose memory would be kept over several flips. The reason why the rigidity length ξ_{rig} is bounded from below by the dynamical heterogeneity length ξ_{dh} is that dynamical rigidity can be assessed only once spins have moved (an immobile block of spins is trivially rigid).

VI. DISCUSSION

A. On our main results

1. Avoided spin-glass criticality

We have seen in Sec. VD that for the model of interacting spins with slowly rearranging couplings, cooperative effects resulting from interactions between spins dominate over purely dynamical heterogeneities in a broad time regime, potentially extending over one decade or more after the relaxation time τ_α . Although cooperative effects are also dynamical here, in the sense that no static spatial correlations are present in the model as discussed in Sec. III, this dynamical cooperativity keeps track of the underlying critical spin-glass physics, which only partly unfolds due to the slow rearrangements of the coupling constants. One might thus speak of an avoided spin-glass transition due to slow rearrangements.

The dynamical rigidity length ξ_{rig} is indeed rooted in the spin-glass transition that would occur in the system for quenched random couplings. In the absence of rearrangements of the couplings, a static spin-glass correlation length would develop. Slow coupling rearrangements suppress static correlations, and turn this static correlation length into the purely dynamic length ξ_{rig} .

2. Landscape picture and restoring forces

We can get a better understanding of this avoided spin-glass transition by using the so-called free energy landscape picture [21]. In our first model where spin interactions play a significant role, there is a high probability that the initial state corresponds to one of the lowest energy states, since the system spans most of its time in these preferred configurations. Imagine now that one of the spins S_{i_0} suddenly flips: this increases the total energy, and as a result there is a high probability that the spin S_{i_0} flips back to its original value to recover the initial low energy. Such a back and forth event is due to the couplings to the neighboring spins which corresponds to *restoring forces* towards the lowest energy states [42]. Let us consider the free energy landscape [21] where the free energy is plotted as a function of an index enumerating the 2^N possible configurations of the spins. According to thermodynamic theories [15,16,57], in supercooled liquids, this landscape is extremely complicated [21], with many low-energy states separated by high barriers. Starting “downhill” (i.e., in a low-energy state), another metastable configuration can be reached only by a thermal jump over the surrounding barriers: such successful jumps are extremely rare, their fraction is as small as $1/(\nu_0 \tau_\alpha) \ll 1$.

In other words, most of the thermal attempts of the system to escape its low-energy state are unsuccessful, because the landscape drives the system back to its original configuration: this amounts to the restoring forces alluded to above. Eventually, the memory of the initial configuration is lost when the slow evolution of the couplings makes the original configuration not so low in energy, favoring the transition to a new low-energy configuration. In our second model, where interactions between spin are absent, such landscape-driven restoring forces cannot exist, and therefore we expect that ξ_{rig} captures only the characteristic length scale ξ_{dh} of dynamical heterogeneities.

3. Multiple length scales at play

It is important to note that no static length is present in the model of interacting spins considered here. Numerically, one finds that both ξ_{dh} and ξ_{rig} go to 1 in the long-time limit (i.e., the lattice spacing, analogous to a molecular size). Analytically, one finds that at equilibrium, all degrees of freedom (spins and couplings) are fully decorrelated; see Sec. III. Hence a point-to-set length evaluated on the spin degrees of freedom would be equal to 1. These results on the present simple model of interacting spins are actually consistent with experimental results on the cubic dielectric response, which recover the ideal gas response in the limit of vanishing frequency. However, note that in more realistic glass models describing interacting particles, the point-to-set length ξ_{PTS} characterizing the nontrivial correlations of particle positions is found to be larger than particle size [22]. This indicates that the relation between the usual point-to-set length based on particle positions and the peak of the nonlinear response of the polarization is at best indirect and would deserve further investigations. Our results show in particular that a peak in the frequency-dependent nonlinear response of the polarization, with a qualitatively correct temperature dependence, can be obtained in a model with no associated point-to-set length.

4. Purely dynamic nature of rigidity

Overall our work illustrates explicitly that the qualitative behavior of nonlinear responses—in temperature and frequency—changes drastically depending on the presence or absence of interactions between effective degrees of freedom for glass formation. In the framework of the simple spin models studied here, this effect has been traced back to the fact that cubic responses are actually not sensitive to dynamical correlation effects (characterized by ξ_{dh}) but rather to dynamical rigidity effects (characterized by ξ_{rig}). One may expect that the same effect carries over to nonlinear responses of higher order. Therefore we interpret the experimental length $\ell_{\text{NonLin}}(T)$ mentioned in the Introduction as being identical to $\xi_{\text{rig}}(T)$, consistently with empirical observations [28–31,35]. Physically, such rigidity effects only exist if interaction terms in the Hamiltonian explicitly make some spin configurations being preferred with respect to other spin configurations, as long as coupling constants have not yet rearranged, i.e., over a long but finite timescale. In that case only, the system has some finite rigidity, i.e., when perturbed by the field, the system will react as a whole (i.e., a superdipole), unless the field

frequency is too small, in which case the superdipoles melt. Interestingly, recent extensive numerical simulations of glass models at low temperature have shown that dynamic facilitation is at play in the late relaxation stage, for times much larger than the characteristic relaxation time τ_α [45,46]. One may thus wonder whether the eventual melting of superdipoles in our model may involve some type of effective dynamic facilitation, whereby coherent domains could progressively rearrange through, e.g., diffusion of their boundaries. Whether dynamic facilitation is involved or not in this late-stage relaxation, the mere existence of superdipoles for a time window extending significantly beyond τ_α is a clear sign of the key role played by interactions.

B. More general KCM

1. Local kinetic constraints alone are not enough

We have considered only a specific KCM, with a specific way to introduce kinetic constraints for the spins, based on a Kob-Andersen type of dynamics. Although we cannot formally exclude the possibility that some other KCM which includes spin degrees of freedom coupled to an external field might have a peak in the nonlinear response χ_{21} , our specific kinetically constrained spin model precisely shows that the presence of local kinetic constraints *alone* is not in itself sufficient to reproduce the peaked shape of the nonlinear response. Additional physical ingredients are needed, and we argue that a key ingredient is the presence of amorphous order, which we have characterized.

2. Plaquette model in an external field

The case of the plaquette model [17,18,58–60] is of interest in this respect, as it suggests that the distinction between models with interactions and models with kinetic constraints may be blurred. Indeed, the plaquette model is a model of interacting spins, but it can be mapped onto a model of noninteracting degrees of freedom through the introduction of effective plaquette variables. However, these two formulations are no longer equivalent when it comes to coupling the spins to an external field. In the plaquette model, the physical variables are the interacting spins, and the plaquette variables correspond to an effective reformulation of the dynamics. The point is that the external field couples to the original spins, and not directly to the plaquette effective variables. While the dynamics of interacting spins can be mapped to the dynamics of noninteracting plaquette variables with kinetic constraints, the coupling of spins with an external field does not translate into a similar simple coupling term of plaquette variables with the external field. One rather has to express a given spin in terms of plaquette variables, which is expected to yield a complicated expression involving (potentially nonlocal) interactions between plaquette variables. Hence, in the presence of an external field, the plaquette formulation also includes (complicated) interactions between plaquette variables, and does not boil down to a simple model of noninteracting degrees of freedom with kinetic constraints.

C. Connections with glass theories

1. Frustration-based scenario of the glass transition

It is of interest to briefly discuss our results in the perspective of existing glass theories. Our finding of an “avoided spin-glass criticality” bears some resemblance with the so-called Frustration Theory of the glass transition in which geometric frustration prevents criticality to fully unfold [16]. In this scenario there is an avoided critical point T^* —with $T^* > T_g$ —around which the order develops only to some finite range. This yields an ever-flowing—though with highly nontrivial correlations—liquid state, and thus an ideal-gas response at zero frequency for nonlinear cubic responses. Another possibility with which our findings are naturally compatible is the unreachable critical point of Random First Order Transition theory inspired from p -spin models [15,57]. According to the RFOT scenario, the static correlation length scale is the point-to-set length ξ_{PTS} (see Ref. [22]), which diverges at the Kauzmann temperature T_K —where $T_K < T_g$. This yields, as well, an ideal gas response at zero frequency for nonlinear cubic response, as anticipated in Ref. [33], because this length scale does not couple directly to a spatially homogeneous external field, such as the one used in dielectric experiments [32,42].

2. Key role of amorphous order

More generally, one may imagine other unknown scenarios that would be compatible both with experimental measurements of nonlinear responses and, at a qualitative level, with the results we obtained on simple spin models. These scenarios should be such that (i) interactions between degrees of freedom play a major role, favoring some configurations which are not spatially periodic, and which are driven by a critical point which cannot be crossed at equilibrium on human timescales, and (ii) there is an ideal-gas response at any order in the applied field at zero frequency, while, at finite frequencies, qualitative differences arise between linear and nonlinear responses. Denoting by “molecular amorphous ordering” any scenario fulfilling points (i) and (ii), one of the outcomes of this work is thus to better illustrate what the nonlinear experiments teach us: namely, the fact that, upon cooling, molecular amorphous order develops [32,35,42]. However, these experiments do *not* allow one to discriminate between some already existing scenarios of molecular amorphous order, and it might be that they turn out to be consistent with yet unexplored ones. Thus, we still have to unveil the microscopic mechanism by which the amorphous ordering—and the associated glass transition—takes place so often in nature.

VII. CONCLUSION

We have performed a numerical determination of the nonlinear, third-order (dielectric) response to an external field in model glass formers explicitly composed of a large number of degrees of freedom, in our case, spins and couplings or mobility excitations. We have shown that a model of interacting spins with slowly rearranging coupling constants was able to reproduce, at a qualitative level, the peaked shape of the nonlinear response as a function of frequency, as well as the

temperature dependence of the nonlinear response rescaled by the corresponding response of noninteracting spins. In contrast, a simple model of noninteracting spins with local kinetic constraints is not able to reproduce the peaked shape of the nonlinear response. Although we cannot exclude that other types of KCM might lead to a peaked shape of the nonlinear response, this result indicates that local facilitation alone, without interactions, is not able to generate the experimentally reported humped shape of the nonlinear response, whereas local facilitation is enough to generate dynamical heterogeneities. Following previous works [33,34], we interpret the humped shape of the nonlinear response as resulting from a local rigidity of the spin dynamics, which involves simultaneously rearranging regions. The heuristic superdipole argument [36,37] takes this physical picture literally and considers rigid blocks of spins that flip coherently, while having a disordered internal structure. In our model of interacting spins, we identify a dynamical rigidity length which quantifies the effective size of coherently flipping spin blocks (i.e., spins that flip together over a relatively short time window). Yet, at odds with the superdipole argument, spin blocks melt at large time due to the slow rearrangement of coupling constants, which may also be viewed as a rearrangement of the local free-energy landscape. This provides a useful characterization of the notion of amorphous order. An important point is that the rigidity of spin blocks can be assessed only after spins have flipped (possibly several times), which is hindered by dynamical heterogeneities of the glassy dynamics. Hence the apparent rigidity length is bounded from below by the length scale of dynamical heterogeneities, meaning that rigidity only becomes visible when it exceeds the length of dynamical heterogeneities.

On the methodological side, a further interest of our work is to propose a relatively simple method to measure the frequency dependence of cubic response in numerical simulations without explicitly applying an ac field. This is made possible by the use of a particular type of nonlinear response, $\chi_{21}(\omega)$, which considers a tiny ac field on top of a small static field E_0 , assuming the ac field to be much smaller than the static one. The nonlinear response $\chi_{21}(\omega)$ has been shown experimentally to behave similarly to other cubic responses that had been considered, like the nonlinear response at frequency 3ω [38,54]. The advantage of the cubic response $\chi_{21}(\omega)$ is that it is linear in the ac field, so that the fluctuation-dissipation theorem can be used to express the ac response in terms of a correlation function of magnetization. Hence the nonlinear response $\chi_{21}(\omega)$ is eventually expressed as the E_0^2 correction to the correlation function of magnetization. In practice, one thus needs only to (carefully) evaluate in numerical simulations the time-dependent correlation function of the magnetization in the presence of a static field. This is much simpler than explicitly applying an ac field at angular frequency ω , measuring the nonlinear response, and repeating the simulations for many different values of ω ranging over several decades. This is an important methodological step in the modeling of glasses, which may foster further studies of nonlinear response in more realistic model glass formers.

We focused here, for the sake of simplicity, on one-dimensional models. Future work should try to characterize the nonlinear response and the corresponding rigidity length

in higher dimensions and in different types of models, to try to confirm that the scenario put forward in this work is robust. In the interacting spin model studied here, the temperature dependence of the characteristic timescale of the rearrangement

dynamics of the couplings was put by hand [see Eq. (4)]. It would be of interest to design more involved models in which the slowdown of the coupling rearrangements would rather emerge from the collective dynamics.

-
- [1] L. Berthier and G. Biroli, Theoretical perspective on the glass transition and amorphous materials, *Rev. Mod. Phys.* **83**, 587 (2011).
- [2] F. Arceri, F. P. Landes, L. Berthier, and G. Biroli, A statistical mechanics perspective on glasses and aging, in *Encyclopedia of Complexity and Systems Science*, edited by R. A. Meyers (Springer, Berlin, 2021), pp. 1–68.
- [3] M. D. Ediger, Spatially heterogeneous dynamics in supercooled liquids, *Annu. Rev. Phys. Chem.* **51**, 99 (2000).
- [4] U. Tracht, M. Wilhelm, A. Heuer, H. Feng, K. Schmidt-Rohr, and H. W. Spiess, Length scale of dynamic heterogeneities at the glass transition determined by multidimensional nuclear magnetic resonance, *Phys. Rev. Lett.* **81**, 2727 (1998).
- [5] P. Lunkenheimer and A. Loidl, Dielectric spectroscopy of glass-forming materials: α -relaxation and excess wing, *Chem. Phys.* **284**, 205 (2002).
- [6] C. Alba-Simionesco, A. Cailliaux, A. Alegría, and G. Tarjus, Scaling out the density dependence of the α relaxation in glass-forming polymers, *Europhys. Lett. (EPL)* **68**, 58 (2004).
- [7] C. Dalle-Ferrier, S. Simon, W. Zheng, P. Badrinarayanan, T. Fennell, B. Frick, J. M. Zanotti, and C. Alba-Simionesco, Consequence of excess configurational entropy on fragility: The case of a polymer-oligomer blend, *Phys. Rev. Lett.* **103**, 185702 (2009).
- [8] M. T. Cicerone and M. Ediger, A new technique for measuring ultraslow molecular reorientation near and below the glass transition, *J. Chem. Phys.* **97**, 2156 (1992).
- [9] G. Li, M. Fuchs, W. M. Du, A. Latz, N. J. Tao, J. Hernandez, W. Götze, and H. Z. Cummins, Light-scattering study of β -relaxation in CaKNO₃ and salol near the liquid-glass transition: Idealized and extended mode coupling theory analysis, *J. Non-Cryst. Solids* **172–174**, 43 (1994).
- [10] A. Aouadi, C. Dreyfus, M. Massot, R. M. Pick, T. Berger, W. Steffen, A. Patkowski, and C. Alba-Simionesco, Light scattering study of the liquid–glass transition of meta-toluidine, *J. Chem. Phys.* **112**, 9860 (2000).
- [11] C.-Y. Wang and M. Ediger, Lifetime of spatially heterogeneous dynamic domains in polystyrene melts, *J. Chem. Phys.* **112**, 6933 (2000).
- [12] E. Vidal Russell and N. E. Israeloff, Direct observation of molecular cooperativity near the glass transition, *Nature (London)* **408**, 695 (2000).
- [13] R. Richert, N. Israeloff, C. Alba-Simionesco, F. Ladieu, and D. L'Hôte, Experimental approaches to heterogeneous dynamics, in *Dynamical Heterogeneities in Glasses, Colloids, and Granular Media*, International Series of Monographs on Physics, edited by L. Berthier, G. Biroli, J.-P. Bouchaud, L. Cipelletti, and W. V. Saarloos (Oxford University Press, Oxford, 2011), pp. 152–202.
- [14] G. Tarjus and D. Kivelson, Breakdown of the Stokes–Einstein relation in supercooled liquids, *J. Chem. Phys.* **103**, 3071 (1995).
- [15] T. R. Kirkpatrick, D. Thirumalai, and P. G. Wolynes, Scaling concepts for the dynamics of viscous liquids near an ideal glassy state, *Phys. Rev. A* **40**, 1045 (1989).
- [16] G. Tarjus, S. A. Kivelson, Z. Nussinov, and P. Viot, The frustration-based approach of supercooled liquids and the glass transition: A review and critical assessment, *J. Phys.: Condens. Matter* **17**, R1143 (2005).
- [17] J. P. Garrahan and M. E. J. Newman, Glassiness and constrained dynamics of a short-range nondisordered spin model, *Phys. Rev. E* **62**, 7670 (2000).
- [18] R. L. Jack, L. Berthier, and J. P. Garrahan, Static and dynamic length scales in a simple glassy plaquette model, *Phys. Rev. E* **72**, 016103 (2005).
- [19] F. Ritort and P. Sollich, Glassy dynamics of kinetically constrained models, *Adv. Phys.* **52**, 219 (2003).
- [20] M. Merolle, J. P. Garrahan, and D. Chandler, Space–time thermodynamics of the glass transition, *Proc. Natl. Acad. Sci. USA* **102**, 10837 (2005).
- [21] A. Cavagna, Supercooled liquids for pedestrians, *Phys. Rep.* **476**, 51 (2009).
- [22] G. Biroli, J.-P. Bouchaud, A. Cavagna, T. S. Grigera, and P. Verrocchio, Thermodynamic signature of growing amorphous order in glass-forming liquids, *Nat. Phys.* **4**, 771 (2008).
- [23] B. Guiselin, G. Tarjus, and L. Berthier, Static self-induced heterogeneity in glass-forming liquids: Overlap as a microscope, *J. Chem. Phys.* **156**, 194503 (2022).
- [24] M. Wyart and M. E. Cates, Does a growing static length scale control the glass transition? *Phys. Rev. Lett.* **119**, 195501 (2017).
- [25] L. Berthier, G. Biroli, J.-P. Bouchaud, and G. Tarjus, Can the glass transition be explained without a growing static length scale? *J. Chem. Phys.* **150**, 094501 (2019).
- [26] G. Biroli, J.-P. Bouchaud, and G. Tarjus, Are defect models consistent with the entropy and specific heat of glass formers? *J. Chem. Phys.* **123**, 044510 (2005).
- [27] D. Chandler and J. P. Garrahan, Thermodynamics of coarse-grained models of supercooled liquids, *J. Chem. Phys.* **123**, 044511 (2005).
- [28] C. Crauste-Thibierge, C. Brun, F. Ladieu, D. L'Hôte, G. Biroli, and J.-P. Bouchaud, Evidence of growing spatial correlations at the glass transition from nonlinear response experiments, *Phys. Rev. Lett.* **104**, 165703 (2010).
- [29] C. Brun, F. Ladieu, D. L'Hôte, G. Biroli, and J.-P. Bouchaud, Evidence of growing spatial correlations during the aging of glassy glycerol, *Phys. Rev. Lett.* **109**, 175702 (2012).
- [30] T. Bauer, P. Lunkenheimer, and A. Loidl, Cooperativity and the freezing of molecular motion at the glass transition, *Phys. Rev. Lett.* **111**, 225702 (2013).
- [31] R. Casalini, D. Fragiadakis, and C. M. Roland, Dynamic correlation length scales under isochronal conditions, *J. Chem. Phys.* **142**, 064504 (2015).

- [32] S. Albert, M. Michl, P. Lunkenheimer, A. Loidl, P. M. Déjardin, and F. Ladieu, Third and fifth harmonic responses in viscous liquids, *J. Stat. Mech.* (2019) 124003.
- [33] J.-P. Bouchaud and G. Biroli, Nonlinear susceptibility in glassy systems: A probe for cooperative dynamical length scales, *Phys. Rev. B* **72**, 064204 (2005).
- [34] M. Tarzia, G. Biroli, A. Lefèvre, and J.-P. Bouchaud, Anomalous nonlinear response of glassy liquids: General arguments and a mode-coupling approach, *J. Chem. Phys.* **132**, 054501 (2010).
- [35] S. Albert, T. Bauer, M. Michl, G. Biroli, J.-P. Bouchaud, A. Loidl, P. Lunkenheimer, R. Tourbot, C. Wiertel-Gasquet, and F. Ladieu, Fifth-order susceptibility unveils growth of thermodynamic amorphous order in glass-formers, *Science* **352**, 1308 (2016).
- [36] F. Ladieu, C. Brun, and D. L'Hôte, Nonlinear dielectric susceptibilities in supercooled liquids: A toy model, *Phys. Rev. B* **85**, 184207 (2012).
- [37] U. Buchenau, Modeling the nonlinear dielectric response of glass formers, *J. Chem. Phys.* **146**, 214503 (2017).
- [38] P. Gadige, S. Albert, M. Michl, T. Bauer, P. Lunkenheimer, A. Loidl, R. Tourbot, C. Wiertel-Gasquet, G. Biroli, J.-P. Bouchaud, and F. Ladieu, Unifying different interpretations of the nonlinear response in glass-forming liquids, *Phys. Rev. E* **96**, 032611 (2017).
- [39] R. Richert and S. Weinstein, Nonlinear dielectric response and thermodynamic heterogeneity in liquids, *Phys. Rev. Lett.* **97**, 095703 (2006).
- [40] A. R. Young-Gonzales, K. Adrjanowicz, M. Paluch, and R. Richert, Nonlinear dielectric features of highly polar glass formers: Derivatives of propylene carbonate, *J. Chem. Phys.* **147**, 224501 (2017).
- [41] R. Richert, Nonlinear dielectric effects in liquids: A guided tour, *J. Phys.: Condens. Matter* **29**, 363001 (2017).
- [42] G. Biroli, J.-P. Bouchaud, and F. Ladieu, Amorphous order and non-linear susceptibilities in glassy materials, *J. Phys. Chem. B* **125**, 7578 (2021).
- [43] T. Speck, Dynamic facilitation theory: A statistical mechanics approach to dynamic arrest, *J. Stat. Mech.* (2019) 084015.
- [44] T. Speck, Modeling non-linear dielectric susceptibilities of supercooled molecular liquids, *J. Chem. Phys.* **155**, 014506 (2021).
- [45] B. Guiselin, C. Scalliet, and L. Berthier, Microscopic origin of excess wings in relaxation spectra of supercooled liquids, *Nat. Phys.* **18**, 468 (2022).
- [46] C. Scalliet, B. Guiselin, and L. Berthier, Thirty milliseconds in the life of a supercooled liquid, *Phys. Rev. X* **12**, 041028 (2022).
- [47] G. Diezemann, Nonlinear response theory for Markov processes: Simple models for glassy relaxation, *Phys. Rev. E* **85**, 051502 (2012).
- [48] G. Diezemann, Higher-order correlation functions and nonlinear response functions in a Gaussian trap model, *J. Chem. Phys.* **138**, 12A505 (2013).
- [49] G. Diezemann, Nonlinear response theory for Markov processes. III. Stochastic models for dipole reorientations, *Phys. Rev. E* **98**, 042106 (2018).
- [50] G. Diezemann, Nonlinear response theory for Markov processes. IV. The asymmetric double-well potential model revisited, *Phys. Rev. E* **106**, 064122 (2022).
- [51] F. Kremer and A. Schönhal, *Broadband Dielectric Spectroscopy* (Springer-Verlag, Berlin, Heidelberg, New York, 2003).
- [52] R. Penney, A. Coolen, and D. Sherrington, Coupled dynamics of fast spins and slow interactions in neural networks and spin systems, *J. Phys. A: Math. Gen.* **26**, 3681 (1993).
- [53] B. Schulz, M. Schulz, and S. Trimper, Mixed mobile ion effect: A numerical study on the basis of a modified two-spin facilitated kinetic Ising model, *Phys. Rev. E* **58**, 3368 (1998).
- [54] D. L'Hôte, R. Tourbot, F. Ladieu, and P. Gadige, Control parameter for the glass transition of glycerol evidenced by the static-field-induced nonlinear response, *Phys. Rev. B* **90**, 104202 (2014).
- [55] L. Berthier and J. P. Garrahan, Numerical study of a fragile three-dimensional kinetically constrained model, *J. Phys. Chem. B* **109**, 3578 (2005).
- [56] E. Bertin, J.-P. Bouchaud, and F. Lequeux, Subdiffusion and dynamical heterogeneities in a lattice glass model, *Phys. Rev. Lett.* **95**, 015702 (2005).
- [57] P. G. Wolynes and V. Lubchenko, *Structural Glasses and Supercooled Liquids: Theory, Experiment, and Applications* (John Wiley & Sons Inc., Hoboken, New Jersey, 2012).
- [58] M. E. J. Newman and C. Moore, Glassy dynamics and aging in an exactly solvable spin model, *Phys. Rev. E* **60**, 5068 (1999).
- [59] R. Jack and J. P. Garrahan, Caging and mosaic length scales in plaquette spin models of glasses, *J. Chem. Phys.* **123**, 164508 (2005).
- [60] S. Franz, G. Gradenigo, and S. Spigler, Random-diluted triangular plaquette model: Study of phase transitions in a kinetically constrained model, *Phys. Rev. E* **93**, 032601 (2016).